Investigation of the Electronic and Magnetic Properties of Mn Doped ZnO Using the FP-LAPW method

T. Rezkallah[1], I. Djabri[1], M. M. Koç[2], M. Erkovan[3], Yu. Chumakov[4] and F. Chemam[1]

[1]*Laboratory of Applied and Theoretical Physics, Matter Sciences Department, University Laarbi Tebessi, Tebessa, Algeria.*

[2]*Department of Physics, Kirklareli University, Kirklareli, Turkey.*

[3]*Nanoscience and Nanotechnology Dept., Sakarya University, Sakarya Turkey.*

[4]Department of Physics, Gebze Technical University, Çayırova, Kocaeli-Turkey

Abstract

We report on the results of the structural, electronic and magnetic properties of ZnO (1x1x1), (1x2x2) in the zincblende (ZB) and rocksalt (RS) phases produced by doping Mn in ZnO structures, considering, for the magnetic interaction between the Mn atoms, both the near and far positions. These are evaluated using density functional theory (DFT). The band gaps of the ZnO semiconductor are calculated by the full potential linearized augmented plane wave (FP-LAPW) method with the local spin density approximation (LSDA) and the modified Becke - Johson (mBJ) potential. The results of the theoretical calculations are compared to the experimental values. The gaps of RS-ZnO are 0.735^{LDA} eV and $2.688^{LDA+mBJ}$ eV. They are comparable to 2.45 eV; in the zincblende phase, the gaps are 0.694^{LDA} eV and $2.946^{LDA+mBJ}$ eV compared to the 3.27 eV experimental value. Both the band gap and the total magnetic moment of Mn doped ZnO increased in the supercell 1x2x2 for the RS and ZB phases**.** Our analysis revealed that the mBJ potential is very efficient for the determination of the band gaps of ZnO semiconductors; it is clear that the mBJ potential gives good results for the treatment of the d-orbitals.

Keywords: Band gap , ZnO, mBJ, supercell ,WIEN2k, FP-LAPW .

PACS: 71.15.Mb, 71.15.-m, 75.50.Pp, 71.20.-b, 68.65.Cd

1. INTRODUCTION

The way to control the electronic semiconductor properties is to introduce a metallic impurity to determine the band gap. The II-VI and III-V group semiconductors, doped with transition metals, may be used in several applications, due to their interesting magnetic properties. These semiconductors are usually called dilute magnetic semiconductors (DMSs) and are supposed to be potential building blocks for spintronic devices **[1]**.

DMSs have attracted attention due to the capability of two compounds of spin and charge to be used as magneto-optical, magneto-electrical and magneto-transport devices **[2-5]**. In diluted magnetic semiconductors the cations are replaced by the magnetic impurity. The replacement causes strong magnetic outcomes on the host materials without deteriorating their electronic and optical properties **[2]**. ZnO doped by a magnetic impurity presents photoelectric and piezoelectric properties in spintronic device applications **[6-8]**.

Recently , great advancements have been achieved in the one-dimensional ZnO based DMSs. Density functional theory (DFT) showed that ZnO is a very good semiconductor for high-T_c ferromagnetic materials (T_c is the Curie temperature). Dietl et al. **[3]** made a Mn-doped ZnO that has high T_c . In experimental work, Fukumura et al. **[09]** investigated the doping of Mn in ZnO, and concluded that a small amount of Mn showed an anti-ferromagnetic exchange coupling. Sharma et al. **[10]** found a ferromagnetic state above room temperature in Mn-doped ZnO and also observed a paramagnetic phase at room temperature. Ueda et al. **[11]** found that ZnO films doped with Co can show ferromagnetic characteristics and high Curie temperature T_c . Sato et al. **[12]** showed, by using ab initio methods, that the anti-ferromagnetic state is observed in Mn doped ZnO and the ferromagnetic state was more stable than with the other transition metals; they suggested that the Cr-doped ZnO is a good candidate for a high Curie temperature ferromagnetic in diluted magnetic semiconductors.

In this paper, we study the effects of Mn on the structural, electronic and magnetic properties of ZnO. It is necessary to use the first-principles methods based on DFT in order to predict the effect of doping before carrying out experimental work. We study both the ferromagnetic (FM) and anti-ferromagnetic (AFM) coupling of spins to show the effect on the structural, electronic and magnetic properties. We believe that our results can supply a theoretical knowledge for the doping approach in order to have control over the structures and the properties of ZnO. The objective of the present study is to provide a guideline for the synthesis of new magnetic materials; this is done by using full potential linearized augmented plane wave (FP-LAPW) calculations.

2. COMPUTATIONAL METHOD AND DETAILS

In this work, we performed a series of calculations to determine the structural, electronic and magnetic properties of Mn:ZB-ZnO and Mn:RS-ZnO using the FP-LAPW method. In this approach, the simulated unit cell is shared by two regions (muffin-tin and interstitial). Calculations have been done in the WIEN2k code **[13]** which is a practical code for the FP-LAPW. In the calculations performed for the interstitial region, the energy cut-off was $k_{max}R_{mt} = 7$, the radius of the muffin tin (RMT) was chosen for Zn and O as 1.5 a.u and for Mn as 1.2 a.u. For energy convergence we used **125** k-points in the special irreducible Brillouin zone (BZ) to obtain very good results. The first-principles calculations are based on the density functional theory (DFT). The total energies were calculated using the full potential linearized augmented plane wave (FP-LAPW) method using the WIEN2k package **[13]**.

3. RESULTS AND DISCUSSION

3.1. Structural Properties

ZnO has the wurtzite, rocksalt (RS) and zincblende (ZB) structures. The rocksalt phase of ZnO has a NaCl cubic structure with lattice parameter **4.271 Å [18]**, the lattice parameter of the zincblende structure of ZnO is **4.62 Å [17]**. We have used the experimental lattice parameters to determine the parameters of the Murnagan equation (EOS); these parameters are summarized in Table 1. The table contains results of this work, previous theoretical calculations and experimental data for comparison. The present results show coherence with the previous experimental and theoretical values. Better results are obtained with the LSDA approximation. Our optimized calculations with the LSDA are shown in Table 1.

In our calculations, the lattice parameter for the rocksalt structure is found to be **a = 4.331 Å ,** which shows a great consistency with the experimental value of **4.271 Å [18] ;** for zincblende, the predicted lattice parameter **a = 4.331 Å** is also in good agreement with the experiment value of **4.62 Å [17]**. The same observation is valid for B0 and B' as well.

In these calculations, the convergence parameter $R_{MT}k_{max}$ was set to 7.0, and to obtain self-consistency **125** k-points (ndiv = 8x4x4) were used in the irreducible wedge of the irreducible Brillouin (IBZ) for the rocksalt and zincblende phases. All these values have been chosen to ensure that the total energy converged to better than **0.001** Ry. The cut-off energy, which defines the separation between the core and valence states, was set to **-9.496** Ry.

For structural properties, the exchange potential was calculated using both the local-density approximation (LSDA) and the modified Becke - Johson (mBJ) potential **[14]**. The Zn-3d and O-2p bands are well separated experimentally, while they partly overlap in the LSDA.

3.2. Electronic properties

The total density of state is calculated using the two approximations LSDA and LSDA+ mBJ, for the two phases of ZnO . The band structure and the total density of states are presented in Figs. 1 and 2.

For the electronic properties of this compound, we studied the total density of states (TDOS) and the band structure. By calculating the band gap, we can find whether the compound is a metal, a semiconductor or an insulator. The band structure is usually calculated in the 1st Brillouin zone of the reciprocal space along special paths connecting high symmetry points. The lowest-energy state above the band gap has the same Γ point as the highest-energy sate below the band gap; this is what we found in Fig. 3, so we can say that ZnO in the ZB phase has a direct gap of 0.694 eV by the LSDA and 2.646 eV by the mBJ. The closest states above and below the band gap do not have the same Γ values. Also we can say that in the RS phase there is an indirect gap of 0.735 eV and 2.688 eV. In Fig. 3, the partial densities of the valence band are attributed to the O-2s and O-2p orbitals, the Zn-d states are dominant in the valence band at the energy range between -6.3 eV to -2.64 eV with the contribution of O-p orbitals. In the top of valence band, between -2 eV to the Fermi level, the O-p states are dominant. The calculated band gaps are summarized in Table 2. The best results are found with the LSDA+mBJ approximation, i.e. the calculated values are closer to the experimental ones (see Table 2.).

3.3. Magnetic properties

The calculations for Mn doped ZnO were performed by using the WIEN2k code **[13]**. In the interstitial space of the unit cell, the RMT values were chosen as 1.5 a.u for zinc (Zn), 1.2 a.u for manganese (Mn) and 1.5 a.u for oxygen (O). We investigate the change in the structural, electronic and magnetic properties of Mn:ZnO for the unit cell of ZnO containing two atoms of Mn with a configuration of (1×2×2). In Figs. 4 and 5, we represent the short and long spin interactions for both the RS and ZB phases (the distance d_{Mn-Mn} is indicated in Table 4). The structure contains 32 atoms of Zn and O doped with 6.25% of Mn atoms. As a result two of Zn atoms were replaced by two atoms of Mn.

The value of our calculated lattice constant for Mn:ZnO is closer to the experimentally measured value of undoped ZnO, a small difference occurs due to the small mismatching in the ionic radii of Zinc and Manganese. To control the modifications of the electronic properties of ZnO, we use the supercell approach. We observe that the values of the gap increased in the RS-ZnO and ZB-ZnO doped with Mn, this type of doping results in a change in the type of structures present. ZnO-doped Mn has a larger gap. The calculated spin polarized density of states of Mn-doped RS- and ZB-ZnO in the short and long distance for the magnetic interaction are shown in Figs. 6 and 7.

The O-s, O-p and Zn-d states are hybridized in a valence band located around -6 eV and -2.5 eV. In ZnO doped Mn, the Mn-d state is hybridized with the Zn-d and O-p states. Between the energy range of -2.5 eV to 0.05 eV only the majority spin (spin up) contribution is present. In the conduction band in the range between 3 eV to 6 eV relative to the Fermi level, this band is built by the O-p states and the spin minority Mn-d states.

The 3d states of Mn are located mainly in the gap and weakly hybridize with the conduction of the Zn 4s, 4p type, leading to a semi-metallic character; the shift of the occupied 3d levels from the Mn to the valence band gives an isolating solution, the partial state density of 3d-Mn is slightly enlarged, and the 3d spin states of the Mn are strongly offset from the top of the valence band **[26]**.

In Table 3, we display the magnetic configuration, the total energy of Mn-doped ZnO in the short and far magnetic spins configurations. The magnetic ground state and the strength of exchange coupling are found for both FM and AFM couplings. The magnetic fundamental state can be determined by the total energy difference of the supercells between the AFM and FM configurations. If the difference of the total energy ΔE is negative, the AFM configuration is observed; in contrast, when ΔE is positive, we have the FM configuration.

As shown in Table 3, the ΔE of the Mn-doped ZnO in the (1×2×2) structure are all negative, which indicates that the AFM states are more stable than the FM states. The AFM coupling gets weaker, when the Mn-Mn bond length increases for a long distance of the exchange interaction (d_{Mn-Mn}= 6.3408 Å); the magnetic exchange interaction is independent of the Mn-Mn distance **[27]**.

In Table 4, all magnetic moments of the Mn atoms are in the ($3.0\mu_B$-$3.2\mu_B$) range; they mainly originate from the 3d electrons of Mn atoms. Oxygen atoms also show a weaker positive value of the spin polarization with the nearest-neighbor Mn atoms, which produces a weak magnetic moment around **0.04- 0.07** μ_B.

For more details on the magnetic coupling of Mn-doped ZnO, we show, in Fig. 7, the total spin polarized density of states for the AFM states. The density of electron spins is asymmetrically distributed; we can see more spin down than spin up electrons.

Lastly, we found the AFM coupling easily in Mn-doped ZnO according to the theoretical analysis, this is in agreement with the experimental work where the AFM coupling in the ZnO-Mn structure is observed **[9,11]**.

4. CONCLUSION

In conclusion, the density functional theory with the FP-LAPW method has been used to evaluate the effects of Mn doping on the physical properties of ZnO in the rocksalt and zincblende phases. The

results show that the presence of Mn, as impurity atoms in ZB-ZnO and RS-ZnO, leads to an increase in the magnetic moment. Moreover, Mn impurity atoms do not significantly change the ZnO lattice parameters, but do cause a large variation in the band gap. Mn:ZnO systems favors anti-ferromagnetism as the fundamental stable state. The observed highly spin polarized conduction carriers indicate that Mn:ZnO in zincblende phase materials have a potential for polarized spin current applications and other spintronic devices.

5. ACKNOWLEDGEMENT

We are grateful to Prof. A. Layadi from the Setif University who has participated in the discussions and correction of this paper.

6. REFERENCES

[1] *D. Benjamin, O. David , J. Pauzauskie, H. Rongrui, and P. Yang, Angew. Chem. Int,* ***45****, 420. 423(2006).*

[2] *H. Ohno. Science, 281, 951-954(1998).*

[3] *T. Dietl , H. Ohno, F. Matsukura, J. Cibert, D. Ferrand. Science,* ***287****, 1019-1022(2000).*

[4] *Z. W. Pai, ZR. Dai, Z. L. Wang. Science,* ***281****, 1947-1949(2001).*

[5] *M. H Huang, S. Mao, H. Feick, H.Q.Yan, Y.Y. Wu, H. Kind, E.Weber, R. Russo, P. D. Yang. . Science,* ***292****, 1897-1899(2001).*

[6] *C. Q.Ye, M. Z. Li, J. Luo, L. F. Chen, Z. M. Tang, J. Pei, L. Jiang, Y. L.Sang, D. B. Zhu. J. Mater. Chem.* ***22****, 4299-4305(2012).*

[7] *R. Chau, B. Doyle, S. Dalta, J. Kavalieros, K. Zhang. Nat. Mater.****6****,810-812(2007).*

[8] *X. Ma, H. Tian. Chem. Soc. Rev.,* ***39****, 70-80(2010).*

[9] T. Fukumura, Z. Jin, M. Kawasaki, T. Shono, T. Hasegawa, S. Koshihara, H. Koinuma, Applied Physics Letters, **78**, 958-960 (2001)

[10] *P. Sharma, A.Gupta, K. V. Rao, Frank J. Owens, R. Sharma, R. Ahuja, J. M. O.Guillen, B. Johansson , G. A. Gehring* Nat.Mat **2**, 673 - 677 (2003)

[11] *K. Uedo, H. Tabata, T. Kawai. Appl. Phys. Lett.****79,****988(2001).*

[12] *K. Sato, H. Katayama-Yoshida, Semicon. Sci. Techno.* ***17****,367(2002).*

[13] *P. Blaha, K. Schwaez, G. K. H. Madsen. D. Kavanicka and J. Luitz. WIEN2k. An Augmented Plane Wave + Local Orbitals Program for Calculating Crystal Properties.Vienna University of Technology. Austria(2014).*

[14] *Perdew, J. Pand , Y. Wang . Phys. Rev. B.****45,****13244(1992).*

[15] *B. Amrani, I. Chiboub, S. Hiadsi, T. Benmessabih, N. Hamdadou, Solid State Commun.* ***137,*** *395(2006).*

[16] *M. Kalay, H. Kart, S. Ozdemin Kart, T. çagin, J. Alloys Compd.* ***484,*** *431 (2009).*

[17] *M. Oshikiri and F. Aryasetiawen, Phys. Rev. B****60,****10754(1999).*

[18] *H. Karzel, W. Potzel, M. Kofferlein,W. Scheiessil, M. Steiner, U. Hiller, G. M., Kalvious, D. W. Mitchell, T. P. Das, P. Blaha, K. Schwarz, M. P. Pastemak, Phys. Rev. B**53,** 11425(1996).*

[19] *S. Desgreniers, Phys. Rev. B**58,**14102(1998).*

[20] *A. Schleife, F. Fuchs, J. Furthmuller, F. Bechstedt. Phys. Rev. B**73,**245212(2006).*

[21] *XB. Chen, L . Qi, MZ . Ma, Q. Jing, G.Li, WK . Wang, RP. Liu. Solid State.Commun;**122,**175(2008).*

[22] *A. Segura, JA. Sans , FJ. Manjon, A. Munoz, MJ. Herrera-Cabrera . Appl. Phys.Lett;**83**,278(2003).*

[23] *Z. Charifi, H. Baaziz , AH . Reshak , Phys.Stat. Sol.(b)**244**(9),3154(2007).*

[24] *YZ. Zhu, GD. Chen, H. Ye, A. Walsh, CY. Moon, SH. Wei. Phys. Rev. B.**77,**245209 (2008).*

[25] *A. Ashrafi, A. Ueta, H. Kumano, I. Suemune. J. Cryst. Growth **221,** 435 (2000).*

[26] *T. Charnier. "Magnetic properties and electronic structure of diluted magnetic semiconductor types II.VI. " doctorate theses (in French) Aix-marseille University I,(2008).*

[27] *F. Zhang , D.Chao, H. Cui, W. Zhang and W. Zhang, nanomaterials **5,**885(2015).*

Figures and Tables captions

Fig. 1: Total density of state (TDOS) and band structures of the RS-ZnO(a;b) and ZB-ZnO(c;d) (1x1x1) monocrystals with different exchange correlation potentials.

Fig. 2: Total density of state (TDOS) and band structures of the RS-ZnO(a;b) and ZB-ZnO(c;d) (1x2x2) supercells with different exchange correlation potentials.

Fig. 3: Partial density of state (PDOS) of the RS-ZnO (a;b) (1x1x1) supercell and ZB-ZnO (c;d) (1x2x2) supercell with the mBJ approximation.

Fig. 4: Schematic overview of the structures of the ZnO supercell (1x2x2) doped Mn in the rocksalt phase for the near (a) and far (b) atoms of the Mn interaction. The colors of the Zn, Mn, O atoms are rose, gray and red, respectively.

Fig. 5: Schematic overview of the structures of the ZnO supercell (1x2x2) doped Mn in the zincblend phase for the near (a) and far (b) atoms of the Mn interaction. The colors of the Zn, Mn, O atoms are rose, gray and red, respectively.

Fig. 6: The calculated spin polarized density of states of Mn:ZnO in the rocksalt phase in the 1x2x2 supercell structure. The DOS along the positive (negative) Y-axis indicates the spin up (spin down) of the DOS .

Fig. 7: The calculated spin polarized density of states of Mn:ZnO in the zincblende phase in the (1x2x2) supercell structure. The DOS along the positive (negative) Y-axis indicates the spin up (spin down) of the DOS.

Table 1: The lattice constants a(Å), bulk modulus B_0 (GPa) and its pressure derivative B' of ZnO in the RS and ZB phases in the (1x1x1) structure.

Table 2: Calculated band gap with different approximations in the rocksalt and zincblende structures for ZnO compared with the experimental and other theoretical results (all values are given in eV).

Table 3: The nature of magnetic coupling with two Mn atoms in the ZnO supercell structure.

Table 4: Magnetic moments calculated for the Mn and O atoms, the Mn-Mn distance, the Mn-O distance, and the magnetic moment of Mn atoms in the RS- and ZB- ZnO doped Mn supercell structure.

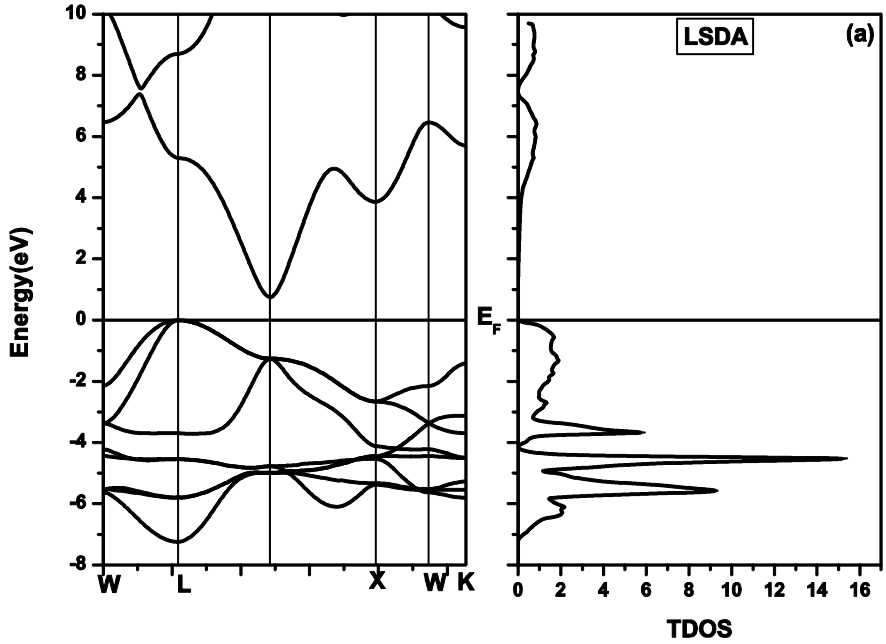
LSDA
(a)
Energy(eV)
E_F
W
L
X
W
K
TDOS

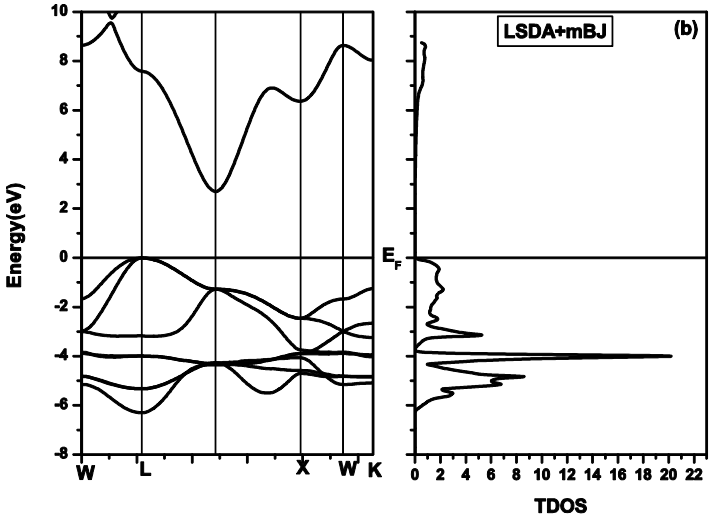
LSDA+mBJ
(b)
Energy(eV)
E_F
W
L
X
W
K
TDOS

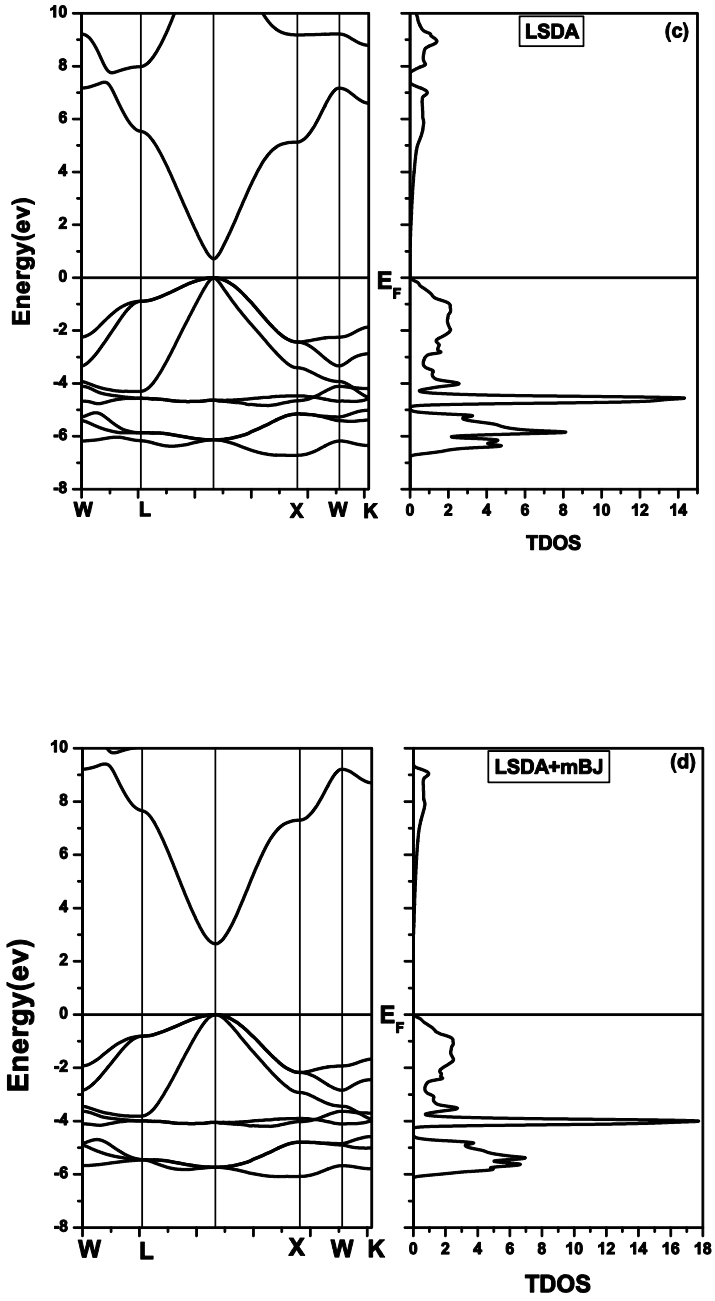

Fig.1: Total density of state (TDOS) and band structures of the RS-ZnO(a;b) and ZB-ZnO(c;d) (1x1x1) monocrystal with different exchange correlation potentials.

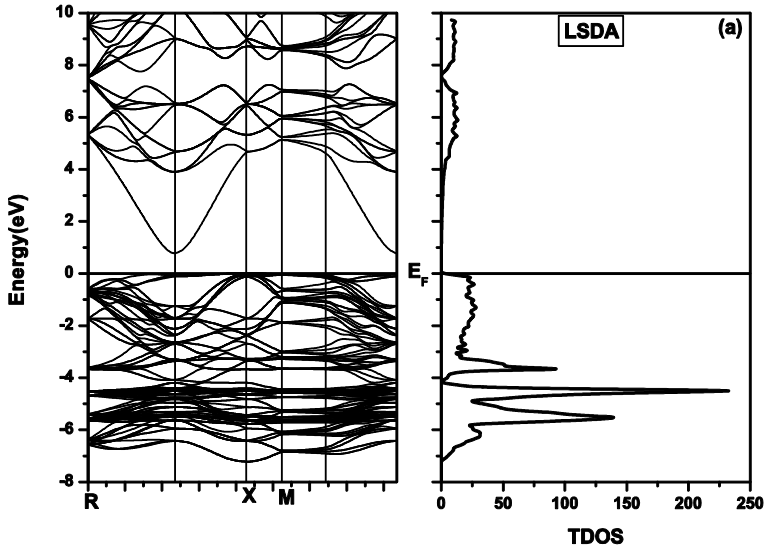
LSDA
(a)
Energy(eV)
E_F
R
X
M
TDOS

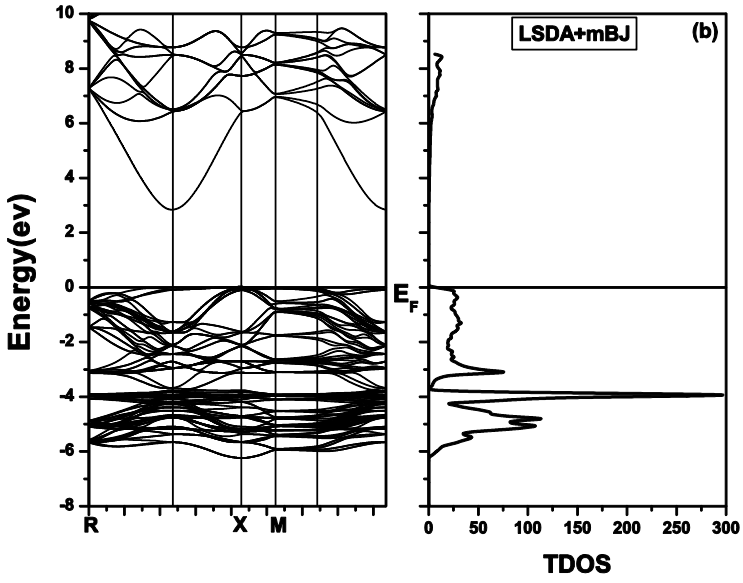
LSDA+mBJ
(b)
Energy(ev)
E_F
R
X
M
TDOS

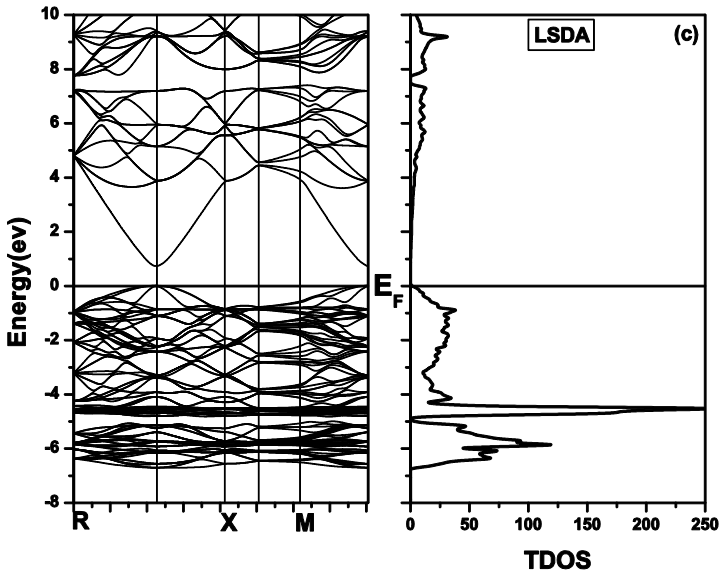

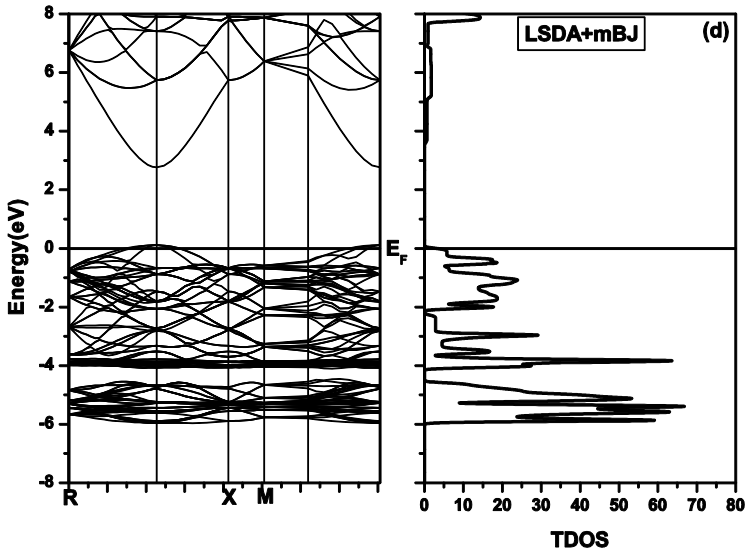

Fig. 2: Total density of state (TDOS) and band structures of the RS-ZnO(a;b) and ZB-ZnO(c;d) (1x2x2) supercells with different exchange correlation potentials.

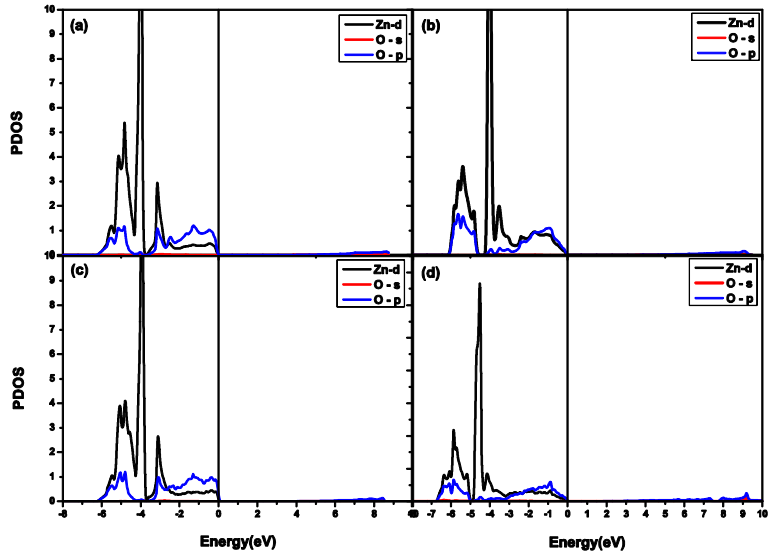

Fig. 3: Partial density of state (PDOS) of the RS-ZnO (a;b) (1x1x1) supercell and ZB-ZnO (c;d) (1x2x2) supercell with the mBJ approximation.

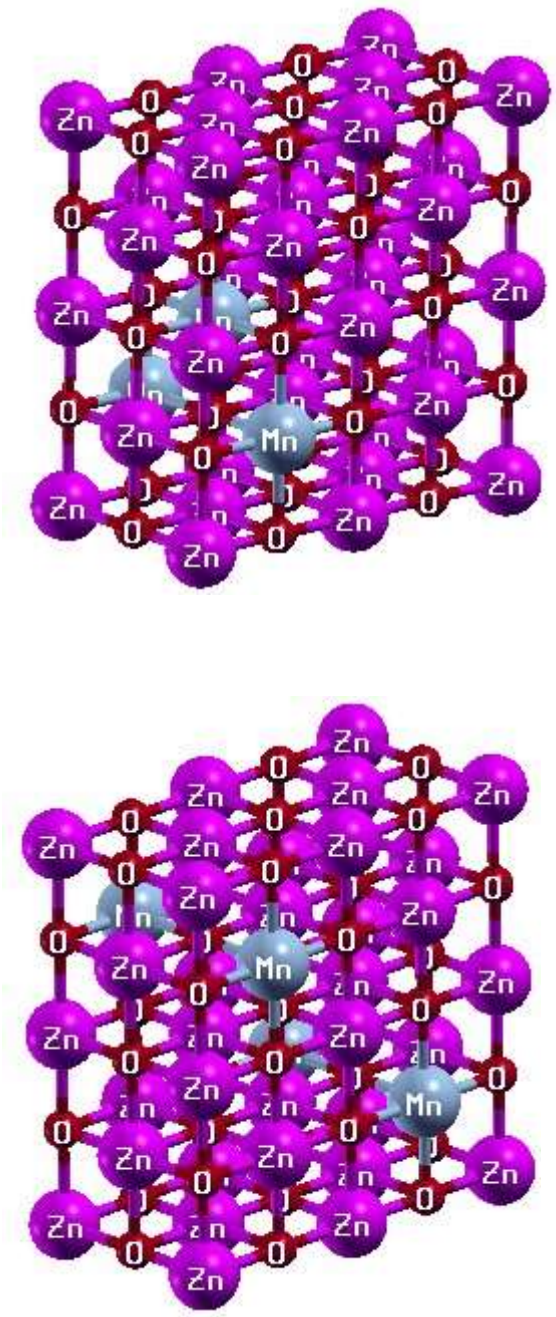

Fig. 4: *Schematic overview of structures of the ZnO supercell (*1x2x2*) doped Mn in the rocksalt phase in short (a) and far (b) atoms of the Mn interaction.* The colors of the Zn, Mn, O atoms are rose, gray and red, respectively.

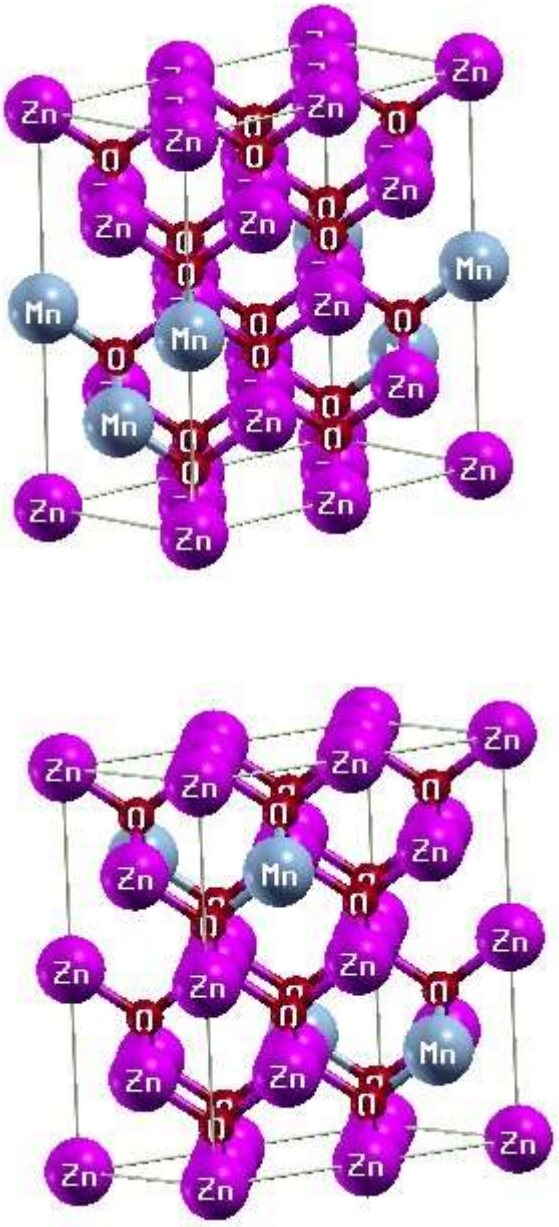

Fig. 5: Schematic overview of structures of the ZnO supercell (1x2x2) doped Mn in the zincblende phase for the neart (a) and far (b) atoms of the Mn interaction. The colors of the Zn, Mn, O atoms are rose, gray and red, respectively.

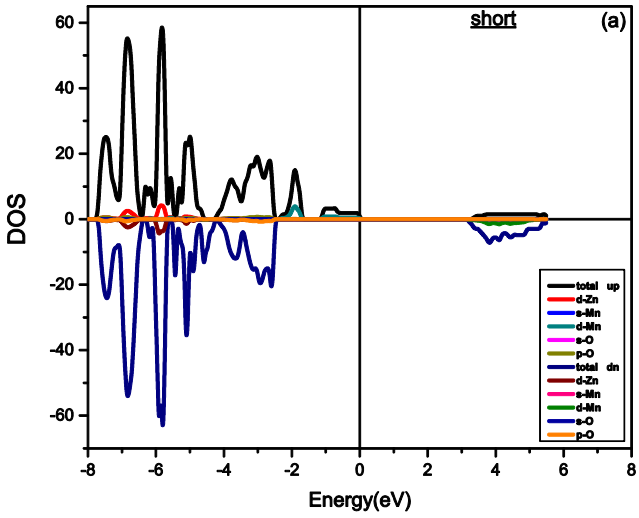

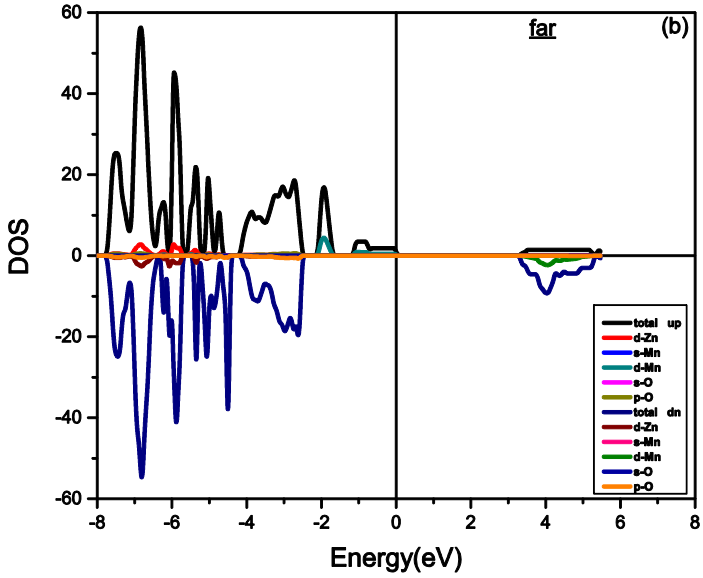

Fig. 6: The calculated spin polarized density of states of Mn:ZnO in the rocksalt phase in the 1x2x2 supercell structure. The DOS along the positive (negative) Y-axis indicates the spin up (spin down) of the DOS .

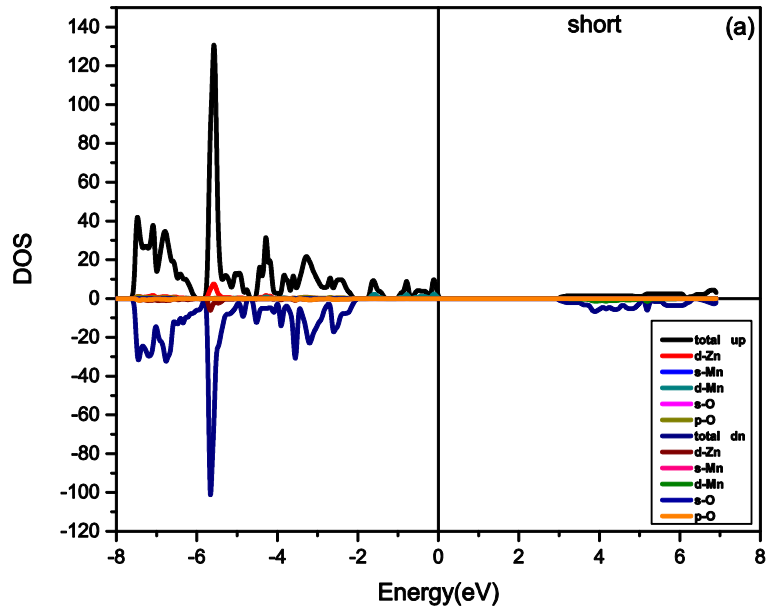

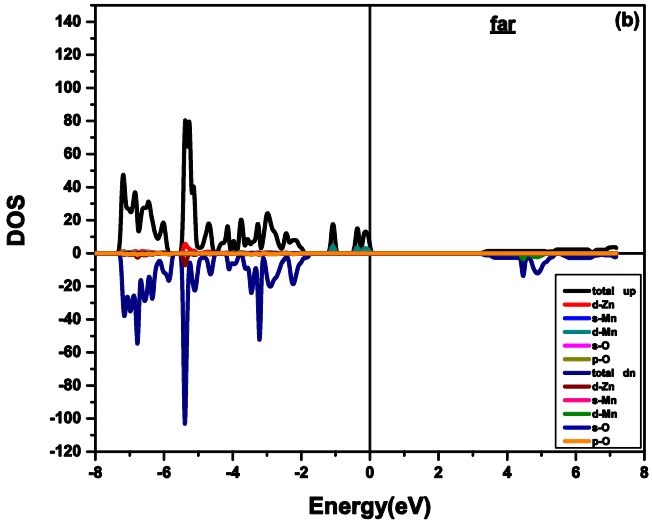

Fig. 7: The calculated spin polarized density of states of Mn:ZnO in the zincblende phase in the (1x2x2) supercell structure. The DOS along the positive (negative) Y-axis indicates the spin up (spin down) of the DOS.

Table 1: The lattice constants a(Å), bulk modulus B_0 (GPa) and its pressure derivative B' of ZnO in the RS and ZB phases in the (1x1x1) structure.

ZB structure	**This work**	**Other theoretical calculations**	**Experiments**
a	**4.4836**	**4.52[a], 4.6329[b]**	**4,62[c]**
B_0	**167.1607**	**168[a] , 139.32[b]**	
B'	**4.8836**	**4.6 [a] , 3.7586[b]**	
RS structure			
a	**4.331**	**4.223[a], 4.3379[b]**	**4.271[d]**
B_0	**201.98**	**209.6 [a], 164.91[b]**	**202[e]**
B'	**4.2927**	**4.46 [a], 4.5318[b]**	**4[d] , 3.54[e]**

[a]Ref.[15] [b]Ref. [16] [c]Ref. [17] [d]Ref. [18] [e]Ref. [19]

Table 2: Calculated band gap with different approximations in the rocksalt and zincblende structures for ZnO compared with the experimental and other theoretical results (all values are given in eV).

	Rocksalt	**Zincblende**
LSDA	**0.735**	**0.694**
LSDA+mBJ	**2.688**	**2.646**
Theoretical calculation	**0.75[A] 1.09[B] 1.1[C]**	**0.65[E] 0.64[A] 0.71[F]**
Exp	**2.45[D]**	**3.27[G]**

[A]Ref. [20] [B] Ref. [21] [C] Ref. [15] [D] Ref. [22] [E] Ref. [23] [F] Ref. [24] [G] Ref. [25]

Table 3: The nature of magnetic coupling with two Mn atoms in the ZnO supercell structure.

	approx	**Configuration**	**E_{FM}(Ryd)**	**E_{AFM}(Ryd)**	**ΔE(Ryd)**	**Nature of Coupling**
1×2×2 RS	**LSDA**	**Near**	**-57237.095**	**-57237.096**	**-0.001**	**AFM**
		Far	**-57237.095**	**-57237.097**	**-0.0002**	**AFM**
	LSDA+mBJ	**Near**	**-57230.786**	**-57231.404**	**-0.618**	**AFM**
		Far	**-57230.786**	**-57230.788**	**-0.002**	**AFM**
1×2×2 ZB	**LSDA**	**Near**	**-57237.381**	**-57237.382**	**-0.001**	**AFM**
		Far	**-57237.388**	**-57237.389**	**-0.001**	**AFM**
	LSDA+mBJ	**Near**	**-57231.3512**	**-57231.404**	**-0.0533**	**AFM**
		Far	**-57231.361**	**-57231.363**	**-0.001**	**AFM**

Table 4: Magnetic moments calculated for the Mn and O atoms, the Mn-Mn distance, the Mn-O distance, and the magnetic moment of the Mn atoms in the RS- and ZB- ZnO doped Mn supercell structure.

	configuration	**d_{Mn-O}(Å)**	**D_{Mn-Mn}(Å)**	**$Mn_1(\mu_B)$**	**$Mn_2(\mu_B)$**	**$O(\mu_B)$**
1×2×2 RS	Near	**2.1595**	**3.0541**	**3.12022**	**-3.12022**	**0.04587**
	Far	**2.1595**	**6.1081**	**3.12053**	**3.12053**	**0.04516**
1×2×2 ZB	Near	**1.9415**	**3.1704**	**3.01477**	**-3.01477**	**0.00175**
	Far	**1.9415**	**6.3408**	**3.00998**	**3.00998**	**0.06406**